

**EXPERIMENTAL STUDY OF STATORS CLOCKING (IN "IGV+CT+R+S" SYSTEM) IMPACT ON  
GASDYNAMIC PERFORMANCES OF FIRST HIGH-LOADED STAGE OF ADVANCED HPC WITH SLOT  
TYPE CASING TREATMENT**

V. Mileschin, N. Savin, A. Petrovitchev, S. Baeva  
Central Institute of Aviation Motors (CIAM)  
2, Aviamotornaya St., 111116, Moscow, RUSSIA  
E-mail: [mileschin@ciam.ru](mailto:mileschin@ciam.ru)

**Abstract**

The results of experimental studies of Stage A-1 - the model of a high-loaded high-pressure compressor (HPC) designed for an engine core demonstrator, with the following design parameters are shown:

$G_{air\ cor}=24.4$  kg/s  $U_{c\ cor}=421$  m/s;  
 $\pi^*=2.28$ ;  $\bar{d}l=0.6623$ .

Three stage versions were tested at CIAM's UV-11 test facility:

- with a smooth lining above the rotor to find an optimal control program for IGV and Stator angles;
- with casing treatment and an optimal control program to expand a stall-free operation range of the Stage;
- with a reduced number of IGV vanes turning in the circumferential direction to study clocking effects in the Stage with a multiple number of vanes in IGV and Stator.

The control program for IGV and Stator vanes was selected. The optimal control program within  $\bar{n}_{cor}=0.6\div 1.05$  provided a high efficiency -  $\eta^*_{ad}=0.88\div 0.89$  at  $\bar{n}_{cor}=0.6\div 0.95$ . The stall margin from the optimal point to stall at  $\bar{n}_{cor}=0.7$  was  $\Delta SM=23\%$ , and then decreased to  $\Delta SM=17\%$  at  $\bar{n}_{cor}=0.95$ ,  $\Delta SM=12\%$  at  $\bar{n}_{cor}=1.0$ .

Casing treatment increased the stall margin by 12% within  $\bar{n}_{cor}=0.6\div 0.9$ .

The clocking effect on efficiency was not high - the difference was 0.7% and was caused by a high axial clearance between the Stage blade rows.

**Terminology**

**Thermodynamic and gasdynamic parameters**

P - pressure, Pa;  
T - absolute temperature, K;  
G - air mass flow, kg/s;  
 $\pi^*$  - total pressure ratio;  
 $\eta^*_{ad}$  - adiabatic efficiency;  
 $H_z=H_z/(U_k^2)$  - expended work factor;  
 $\bar{H}_T=H_T/(U_k^2)$  - theoretical work factor;  
 $\Delta SM$  - stall margin.

**Geometrical parameters**

R1, R2 - Stage 1 and Stage 2 rotors;  
S1, S2 - Stage 1 and Stage 2 stators;  
IGV - inlet guide vanes;  
CT - casing treatment;  
 $\bar{h}$  - blade aspect ratio;  
v - clocking parameter;  
D, R - diameter, radius, m;  
Z - number of blades in a row.

**Kinematic parameters**

n - rotational speed, rpm;  
U - tip speed, m/s;  
C - absolute flow velocity (in the fixed coordinate system), m/s;  
W - relative flow velocity.

**Subscripts**

st - stage;  
R - rotor;  
S - stator;  
h - hub;  
cor - corrected;  
opt - optimal;  
ad - adiabatic;  
max - near choking;  
min - near the stall line.

## Introduction

This work represents the results of "passive" unsteady flow control methodologies developed for high-loaded advanced HPC stages. Among others such methodologies include casing treatment, installed over rotors and stators [1-4].

CIAM has a long-time experience in high-efficient slot type casing treatments developed for the surge margin increase by 4-6% and efficiency - by 0.5÷1.5% within the total operating range [5]. Moreover, investigations of stators clocking in high-loaded stages showed high potential of this technique in terms of efficiency increase by 0.7÷1.8% [6].

This work demonstrates an attempt to combine both abovementioned methodologies of unsteady flow control in high-loaded supersonic HPC stages aiming at flow pulsation reduction and accumulation of their effects on the efficiency [7,8]. Experimental investigations are carried out with a high-loaded Stage A1 with  $\pi^*c=2.28$  pressure ratio. The CIAM's high-loaded Stage K-11 is used as a baseline (a prototype) for Stage A1 development [9]. Clocking effects in this work are studied in accordance with concepts and results published in [1,2] and [10-14].

For clocking effect study Stage A1 is equipped with a special mechanism to turn the stator vanes relative to the inlet guide vanes.

### 1. Test assembly and measurements

Stage A-1 - the first stage of HPC designed for an engine core demonstrator - provides the following parameters: corrected air flow -  $G_{air\ cor.} = 24.4$  kg/s; total pressure ratio -  $\pi^* = 2.28$ ; rotor total pressure ratio -  $\pi^*_R = 2.402$ ; total pressure recovery ratio in IGV -  $\sigma^*_{IGV} = 0.9954$ ; total pressure recovery ratio in Stator -  $\sigma^*_S = 0.9847$ ; flow angle at the rotor inlet -  $\alpha_1 = 89^\circ$ ; flow angle at the

stator outlet -  $\alpha_4 = 69^\circ$ ; rotor inlet outer diameter -  $D_{C1} = 0.55567$  m; relative hub diameter at the rotor inlet -  $\bar{d}_1 = 0.6623$ ; design value of corrected tip speed -  $U_{c.cor} = 421.23$  m/s; design value of flow coefficient -  $\bar{C}_{1a} = 0.396$ ; theoretical work factor -  $\bar{H}_T = 0.507$ .

The stage includes three rows: IGV ( $Z=37$ ,  $\bar{h}=2.42$ ), Rotor - blisk ( $Z=29$ ,  $\bar{h}=0.81$ ), and Stator ( $Z=58$ ,  $\bar{h}=1.11$ ). IGV and Stator vanes are variable ( $\Delta\theta_{IGV} = -33^\circ \div +3^\circ$  and  $\Delta\theta_S = -15^\circ \div +3^\circ$ ).

Fig. 1 shows the Stage A-1 flow passage (with casing treatment).

The test unit with a one-piece ring without CT was assembled with the following clearances between stator and rotor parts: rotor tip clearance along a talc surface was 0.65-0.7 mm ( $\bar{s} = 0.7 \div 0.75\%$ ); tip clearance between rotor blade tips and the hub at the design value of the stator vane angle was 0.6 - 0.75 mm for the leading edge and 1.0 - 1.5 mm for the trailing edge.

Stage A1 was assembled with above-mentioned clearances for tests without CT to study the clocking effect.

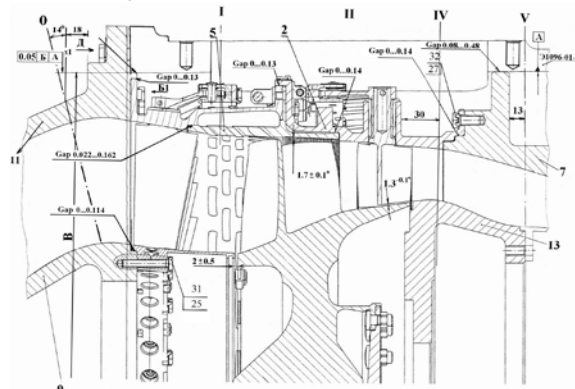


Fig. 1. Stage A-1 flow passage and sections (0; I; II; IV; V) for instrumentation

Air flow was measured by an inlet measuring orifice ( $\varnothing 320$  mm). Fig. 1 shows typical cross-sections from 0-0 to V-V for installation of instrumentation used in tests of the stages.

Seventy pitot tubes forming 7 total pressure rakes (10 in each rake) located in 7 radii were installed in IV-IV section. Six tubes (3 at the tip and 3 at the hub) were installed on walls of the flow passage for static pressure measurements in this section. Single-row, three-row and seven-row) thermocouples were installed in V-V section: total number of thermocouples was 28 installed in 7 rows (4 temperature pickups in each row). The installation diagram of total pressure rakes and thermocouples is shown in Fig. 2.

Table 1. Installation of pitot tubes in IV - IV section

Rake No.	R, mm	$\alpha^\circ$ rel. to the axis	Tube No.	Spacing t, mm	H from the tip	H from the hub
7	264.9	31	21-30	5.78	3.5	
6	259.5	29	21-30	5.66	8.9	
5	253.5	28	21-30	5.53	14.9	
4	247.5	28	31-40	5.4	20.90	
3	241.5	27	41-50	5.27	26.9	
2	235.5	26	51-60	5.14	32.9	
1	230.1	26	61-70	5.02		3.5

The static pressure pickups were installed in the same sections as total pressure pickups.

The measurement accuracy in tests at the test facility is shown in Table 2.

Table 2.

Parameter	Measurement range	Measuring device	Measurement error
Torque	0÷70kg*m	Torque meter	±0.5% of measured value
Pressure	-50÷150 KPa	IKD-27DF	±0.3% of measured value
Temperature	-20÷+100°C	Chromel-copel thermocouples	±2.5°
Rotational speed	2000÷20000 rpm	ELURA	±0.2% of measured value
Air flow	7÷12 kg/s	Flow meter (RMK, Ø320 mm)	±0.5% of measured value
Pressure pulsation	0÷100 kHz	Fast-response «Kulite» sensors	10% of measured value

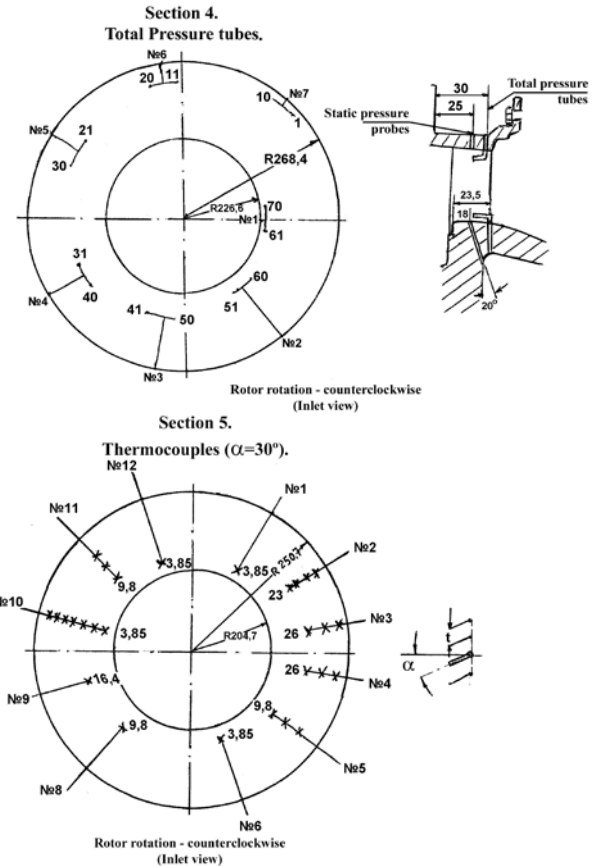


Fig. 2. Installation diagram for pitot tubes and thermocouples

## 2. Choice of IGV and Stator control program

### 2.1 Debugging of IGV and Stator control program

In accordance with the test program, parameters were measured at CIAM's test facility to find an optimal control program for Stage A-1 IGV and Stator vanes. In particular, in addition to target performances at  $\bar{n}_{cor}=0.7$ ,  $\Delta\theta_{IGV}=-30^\circ$  and  $\Delta\theta_S=-12^\circ\pm 3^\circ$ , performances were measured at  $\Delta\theta_{IGV}=-30^\circ$  and  $\Delta\theta_S=-6^\circ$  (see Fig. 3). As can be seen from this figure, an increase in the angle from  $\Delta\theta_S=-12^\circ$  to  $\Delta\theta_S=-6^\circ$  results in an increase in air flow by 13% (from  $G_{cor}=11.5$  kg/s to  $G_{air cor}=13.0$  kg/s) and efficiency by 7% (from  $\eta^*_{ad}=0.85$  to  $\eta^*_{ad}=0.91$ ). Moreover, there is an increase in the stall margin relative to optimal points of performances - from  $\Delta SM=7\%$  to  $\Delta SM=20\%$

Fig. 4 shows performances at  $\bar{n}_{cor}=0.9$ . In addition to performances at  $\Delta\theta_{IGV}=-20^\circ$  and  $\Delta\theta_S=-8^\circ\pm 3^\circ$ , performances at  $\Delta\theta_{IGV}=-20^\circ$  and  $\Delta\theta_S=-2.5^\circ$  were measured. The same pattern was observed - an increase in the angle from  $\Delta\theta_S=-8^\circ$  to  $\Delta\theta_S=-2.5^\circ$  resulted in an increase in efficiency and air flow. Moreover, there was an increase in the stall margin relative to optimal points of performances - from  $\Delta SM=9.4\%$  to  $\Delta SM=18.8\%$ . The stage performances at  $\Delta\theta_{IGV}=-20^\circ$  and  $\Delta\theta_S=-5^\circ$  were measured twice. The second measurement showed a decrease in efficiency and max. air flow by 1%. The difference was caused by inaccuracy of the stator vane angle.

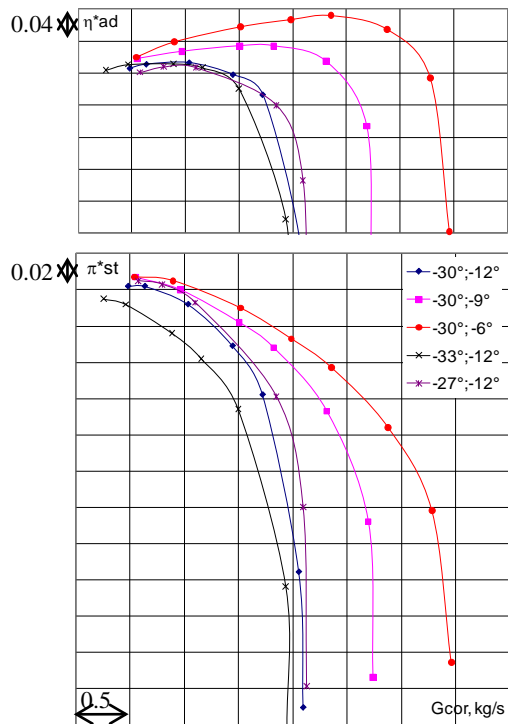


Fig. 3. Stage A-1 performances at  $\bar{n}_{cor}=0.7$  and various  $\Delta\theta_{IGV}$  и  $\Delta\theta_S$

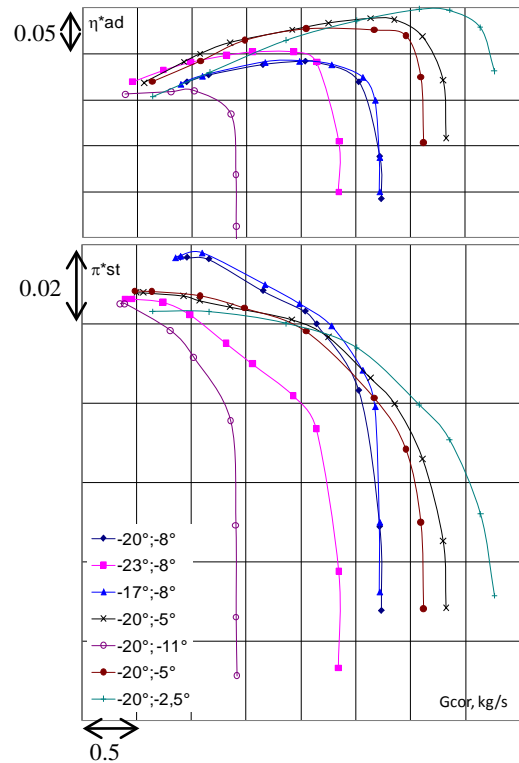


Fig. 4. Stage A-1 performances at  $\bar{n}_{cor}=0.9$  and various  $\Delta\theta_{IGV}$  and  $\Delta\theta_S$

## 2.2 Stage A-1 performances with an optimal IGV and Stator control program

The analysis of measured data at  $\bar{n}_{cor}=0.7$  and  $0.9$  shows that it is reasonable to decrease the angle of stator vanes to reach higher values of efficiency and stall margin. Initially it was proposed to provide the angle of stator vanes according to the law:  $\Delta\theta_S=0.4\Delta\theta_{IGV}$ .

Based on experience in application of the first high-loaded stage in the experimental HPC as well as test results of Stage A-1 at  $\bar{n}_{cor}=0.7$  and  $0.9$ , there are good reasons to provide the angle of stator vanes according to the law:  $\Delta\theta_S=0.25\Delta\theta_{IGV}$ .

Table 3 shows the selected optimal control program for Stage A-1 IGV and Stator. The summarized graph of performances for the optimal control program is shown in Fig. 5. All performances are measured within a wide range - from

a vertical branch to the stall line.

Table 3.

$\bar{n}_{cor}$	$U_{c\ cor}$ , m/s	$\Delta\theta_{IGV}$	$\Delta\theta_S$
0.6	252.7	-30°	-7.5°
0.7	294.9		
0.8	337.0		
0.9	379.1	-20	-5
0.95	400.2	-10	-2.5
1.0	421.2	0	0
1.05	442.3	0	0

A positive  $\pi^*/G_a$  slope angle is observed for most of Stage A-1 performances in the area to the left of max. efficiency, but without losses in the stall margin. There is a smooth increase in static pressure ratio with throttling, that leads to retention of stable operation till stall.

Optimal control of IGV and Stator vanes is beneficial for high efficiency equal to  $\eta^*_{ad}=0.88\div 0.89$  within  $\bar{n}_{cor}=0.6\div 0.95$ .

Stall margin from the optimal point to stall is  $\Delta SM=23\%$  at  $\bar{n}_{cor}=0.7$ , and then decreases to  $\Delta SM=17\%$  at  $\bar{n}_{cor}=0.95$ , and equals to  $\Delta SM=12\%$  at  $\bar{n}_{cor}=1.0$ .

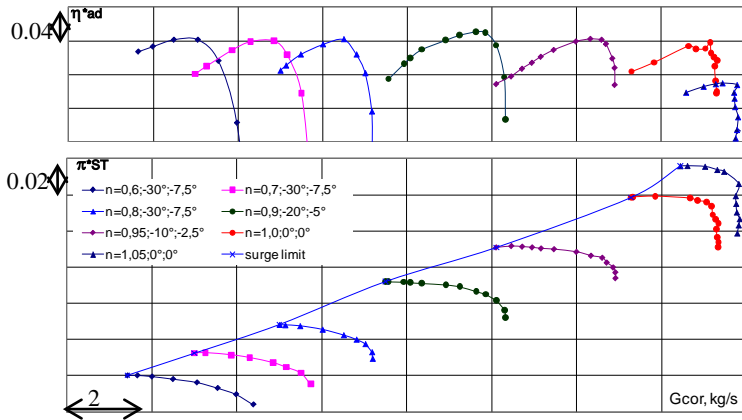


Fig. 5. Stage A-1 performances, at  $\bar{n}_{cor}=0.6 - 1.05$ , IGV and Stator optimal angles

Distributions of Stage A-1 main parameters ( $\pi^*_{st}$ ,  $\Delta T^*/T^*1$  and  $\eta^*_{ad\ st}$ ) along the radius downstream the A-1 Stage at optimal points of performances are plotted in Fig. 6.

Relative hub diameter at the measurement section is equal to  $\bar{d}1=0.8443$ . It is worth to note the following peculiarities of these distributions:

- total pressure ratio is practically constant along the blades height and slightly decreases in hub direction;
- stage efficiency is maximal in the area of hub ( $\eta^*_{ad\ st}=0.9\div 0.95$ ) and decreases in tip direction - up to  $\eta^*_{ad\ st}=0.65\div 0.7$ .

Indicated peculiarities of flow parameters radial distributions comply with the Specification requirements.

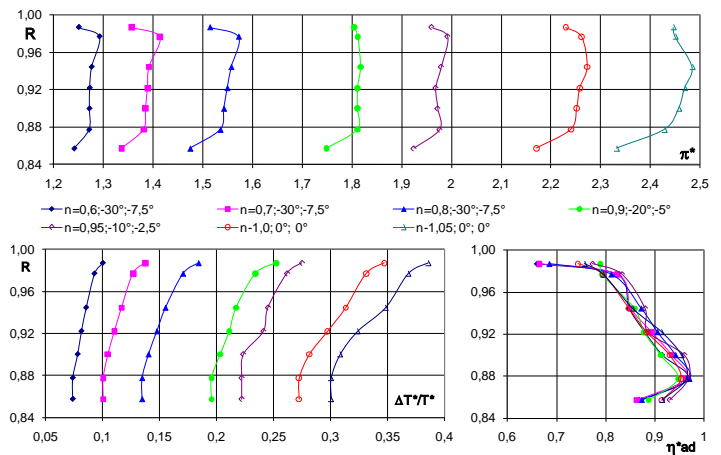


Fig. 6. Distribution of Stage A-1 performances along the radius at optimal points of performances with optimal IGV and Stator control program.

### 3. Test results for the stage with casing treatment

The combined-type casing treatment (CT) used in Stage A-1 tests is shown in Fig. 1. Performances of the stage with CT are measured within  $\bar{n}_{cor}=0.6\div 0.95$  with the selected optimal control program for stator vanes as shown in Fig. 7 for comparison with performances of the Stage with a smooth lining.

Fig. 7 shows that Stage A-1 with CT provides an unexpected increase in stall margin -  $\Delta SM$

increases by ~12% within  $\bar{n}_{cor}=0.6\div 0.9$ .

A considerable increase in efficiency up to  $\eta^*_{ad}=0.92$  (by 3-4% as compared with a smooth rotor casing) is an additional unexpected result for the stage with CT. This extraordinary high gain in efficiency caused by CT application in other experimental stages has not been observed yet.

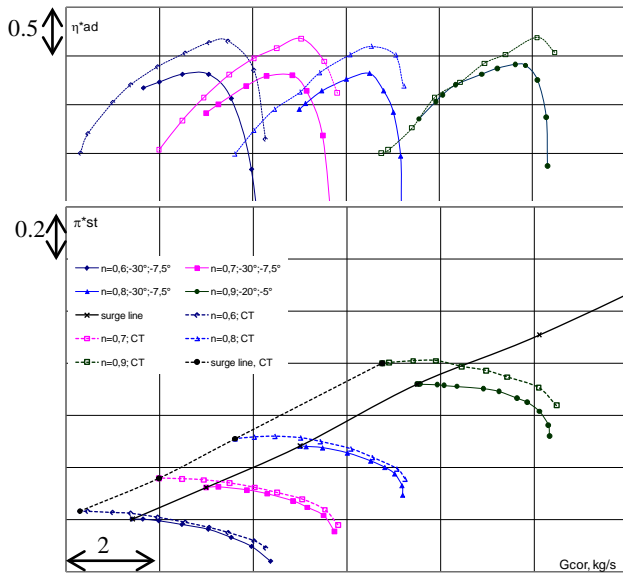


Fig. 7. Performance of Stage A-1 + CT versus a smooth rotor casing

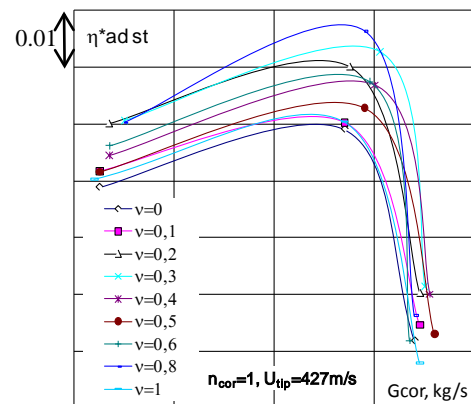
Radial distributions of total pressure, total temperature, and efficiency based on measurements at the Stage outlet can't be clearly associated with flow restructuring in the Stage with CT.

#### 4. Test results for the Stage with various IGV and Stator clocking positions

One way to improve parameters of a three-row stage (stator-rotor-stator) is unsteady interaction control of relatively rotating rows by optimization of relative circumferential positions of stator vanes. High pressure pulsations, velocity circulations and aerodynamic forces are observed in rotor blades under action of flow distortions at the inlet caused by wakes at the IGV outlet as well as potential flow distortions caused

by stator vanes at the outlet. Thus, the rotor is in conditions of interference of two distortion fields propagating downstream and upstream. The distortion level depends on loading of rows and axial clearances between them; the result of their interference depends on the phase difference between synchronous distortions, i.e. IGV-Stator relative circumferential position (clocking). A noticeable effect is achieved for equal or multiple numbers of stator vanes in stator rows, where a considerable portion of distortions has a synchronous effect on rotor blades.

At present, the clocking effects have been experimentally checked in many stages of various types. It is found that optimization of IGV-Stator clocking positions [1-4] improves the stage efficiency by 1.5-2.0%, decreases pressure pulsations in rotor blades by approx. 2 times, and decreases tonal noise by 5-6 dB. For example, Fig. 8 shows Stage K-11 performances (very similar to Stage A-1 [9]) at different IGV-Stator clocking positions. As can be seen from this figure, the difference in efficiency as a function of  $v$ -parameter, which specifies the relative IGV-Stator position, is 1.7%.



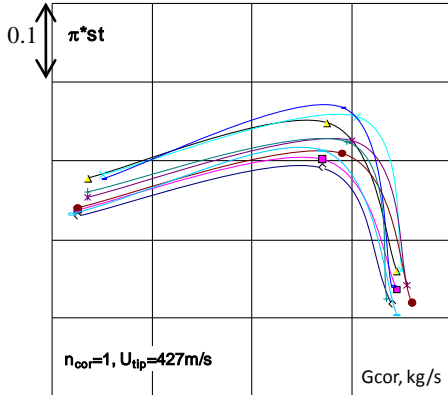


Fig. 8. Performances of Stage K-11 (prototype of Stage A-1) at different IGV-Stator relative positions

For a potential improvement of Stage A-1 performances by controlling the specified clocking effects in this series of tests we used a new IGV with a less number of vanes -  $Z_{IGV}=29$  versus  $Z_{IGV}=37$  in the original IGV version. Consequently, the number of IGV vanes was 2 times less than the number of Stator vanes ( $Z_S=58$ ). In addition, to change IGV and Stator clocking positions, the Stage structure provided an option for IGV circumferential displacement relatively to the fixed Stator to discrete controlled positions during testing. The measuring system in tests of clocking effects was added by fast-response sensors for pressure pulsation measurements installed on a smooth (w/o CT) tip casing at the Rotor inlet and outlet.

For comparison, Fig. 9 shows the Stage A-1 performances measured in tests of Stage A-1 when the number of IGV vanes is  $Z_{IGV}=37$  with smooth lining over the rotor (see Fig. 5).

Fig. 9 shows that the reduced number of IGV vanes (from 37 to 29) in the Stage in clocking tests with unchanged other geometrical parameters and control of IGV and Stator leads to the following changes in Stage A-1 performances:

- there is a shift in performances towards higher air flow at high rotational speeds ( $\bar{n}_{cor}=0.95\div 1.05$ );

- there is an increase in max. efficiency at high rotational speeds (at  $\bar{n}_{cor}=0.9\div 1.05$ ) and a decrease at low rotational speeds (at  $\bar{n}_{cor}=0.6\div 0.8$ );

- Stall line is unchanged at decreased rotational speeds (at  $\bar{n}_{cor}=0.6\div 0.9$ ) and progressively shifts towards lower stall margins with an increase in rotational speeds.

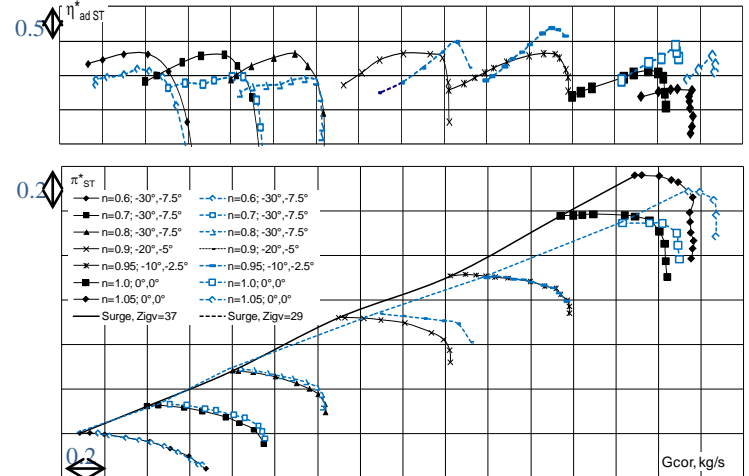


Fig. 9. Stage A-1 performances for assemblies with a smooth casing and  $Z_{IGV}=37$  or  $Z_{IGV}=29$  in studies of clocking effects.

Design parameters of the stage:  
 $U_{C\ cor}=421$  m/s,  $G_{cor}=24.4$  kg/s,  
 $\pi^*_{st}=2.28$ ,  $\pi^*_{ad}=0.875$ .

These noticeable changes in the Stage performances with relatively small changes in its geometrical parameters (reduction in the number of IGV vanes from 37 to 29) indicates a high sensitivity of Stage A-1 to any measures aiming at improvement of Stage parameters. This conclusion is supported by considerable changes in performances of the Stage with CT (see Fig. 7).

Unlike conventional tests of stages for measurements of their gasdynamic characteristics, the experimental studies of clocking effects are more time-consuming, because any point should be measured at different selected IGV-Stator relative circumferential positions. To reduce test time,

clocking effects in these experiments were checked only at three specific air flow points -  $(G_{cor})_{max}$ ,  $(G_{cor})_{opt}$  and  $(G_{cor})_{min}$  to measure the Stage performances at 3 rotational speeds ( $\bar{n}_{cor}=1.0, 0.9, 0.7$ ) and 13 IGV-Stator relative circumferential positions equally spaced within IGV pitch. The pitch angle for 29 IGV vanes was  $\phi_{IGV}=12.4^\circ$ ; the IGV circumferential displacement within this pitch was provided every  $\Delta\phi=1.033^\circ$ , first and last IGV positions were the same relative to Stator vanes. The dimensionless parameter ( $v_i=\Delta\phi_i/\phi_{IGV}$ ) describing IGV/Stator relative position varied from  $v=0$  (initial IGV/Stator position) to  $v=1$  with  $\Delta v=0.17$  increment.

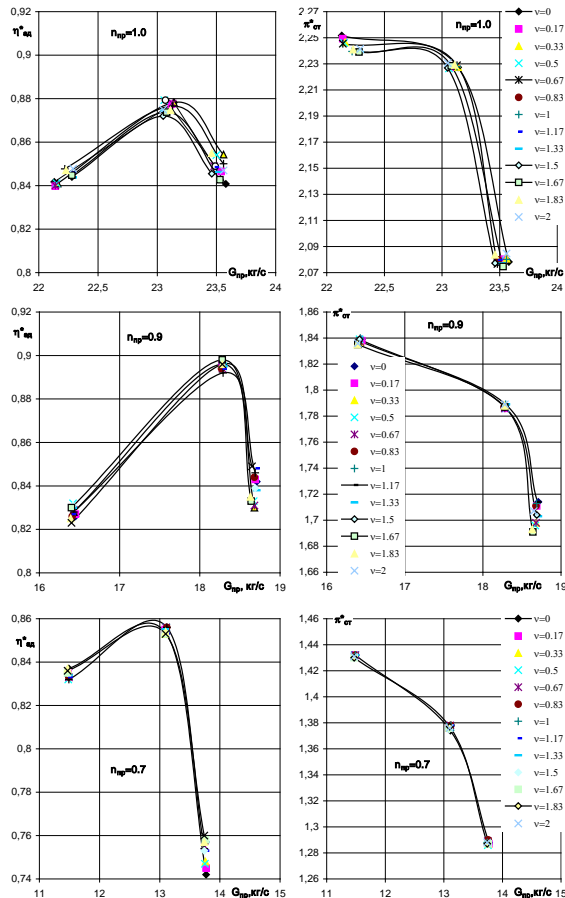


Fig. 10. Performances of Stage A-1 with different IGV/Stator clocking positions as drawn at 3 rotational speeds for 3 airflow points

Fig. 10 shows performances of Stage A-1 with different IGV-Stator clocking positions as drawn for 3 airflow points. There is a clear spread in values of  $\eta^*_{ad}$  and  $\pi^*_{st}$  as a function of  $v$ . Max. efficiency as a function of  $v$  changes by  $\sim 0.7\%$  at  $\bar{n}_{cor}=1.0$ ; this difference is lower with a decrease in  $\bar{n}_{cor}$  and almost absent (within a measurement accuracy) at  $\bar{n}_{cor}=0.7$ . It is also obvious that clocking effect on efficiency depends on positions of a point on the Stage air flow characteristic and achieves higher values in the right branches of the characteristic and lower values near the stall line. The stall line is not variable with changes in IGV-Stator clocking positions.

The comparison of data relevant to an effect of a relative IGV-Stator relative circumferential position on efficiency of Stage A-1 and its prototype - Stage K-11 shows (see Fig. 8 and Fig. 10) that the difference between the characteristics for Stage A-1 is considerably less than for Stage K-11. In particular, maximum efficiency of Stage A-1 at  $\bar{n}_{cor}=1$  changes by 0.7% as a function of  $v$ , whereas efficiency of Stage K-11 changes by 1.7%. As predicted by theoretical studies [1-2], clocking effects in Stage A-1 are relatively lower due to increased axial clearances between rows, in particular, between IGV and Rotor. As a result of control under unsteady interactions between blade rows, the axial clearances are decreased due to a decrease in periodic distortions at the rotor inlet and outlet.

As compared with Stage K-11, a relatively negligible effect of stator clocking position on gasdynamic performances of Stage A-1 is caused by increased axial clearances between rows, especially between IGV and Rotor.

Table 4 shows absolute and relative values of front S1 (between IGV and Rotor) and rear S2



(between Rotor and Stator) axial clearances in the middle radius of the flow passage for Stage A-1 and Stage K-11. The relative values of clearances are found in relation to the axial projection of the rotor in the mid-radius. It is clear that relative axial clearances in Stage A-1 are almost 5 times higher at the Rotor inlet and 3 times higher at the Rotor outlet than in Stage K-11. As a result of control under unsteady interactions between rows by stator clocking in Stage A-1, the axial clearances are decreased due to a decrease in periodic distortions at the rotor inlet and outlet.

Table 4.

	Stage	S1 mm	$b_{ax}$ mm	S2 mm	S1/ $b_{xc}$	S2/ $b_{ax}$
1	K-11	9	71	8	0.13	0.11
2	A-1	44	70	22	0.63	0.31
3	HPC-1	14	39	12	0.36	0.31
4	HPC-2	12	33	10	0.36	0.30

Two bottom lines in Table 4 show absolute and relative values of axial clearances between stator and rotor blade rows in the mid-radius of a two-stage HPC [4]. Third line shows axial clearances between Rotor 1 and Stator 1 (S1) and between Stator 1 and Rotor 2 (S2), i.e. those axial clearances that determine the clocking effects in HPC when changing the relative circumferential positions of Rotor 1 and Rotor 2 blade rows. In this case the relative values of axial clearances are found relatively to Stator 1 axial projection ( $b_{ax}$ ), i.e. to the row located between R1 and R2. Forth line shows axial clearances between Stator 1 and Rotor 2 (S1) and between Rotor 2 and Stator 2 (S2), i.e. those axial clearances that determine the clocking effects in HPC when changing the relative circumferential positions of Stator 1 and Stator 2. In this case the relative values of axial clearances are found relatively to Rotor 2 axial projection ( $b_{ax}$ ), i.e. the row located between Stator 1 and Stator 2.

As can be seen in Table 4, the relative values of axial clearances between blade rows in HPC are similar and rather high (0.3-0.36), i.e. significantly higher than in Stage K-11. Therefore, you should not anticipate considerable changes in HPC gasdynamic characteristics with changes in relative circumferential positions of rotors or stators. The HPC design provides a potential for an increase in axial clearances between Stator 1 and Rotor 2 by 25 mm and should result in a noticeable decrease in unsteady interactions between these rows and negligible clocking effects when changing the relative circumferential positions of Rotor 1 and Rotor 2 blade rows.

Thus, the results of experimental studies of Stage K-11 and Stage A-1 with different relative circumferential positions of stator rows show that for the same or multiple numbers of vanes in stator rows and  $\bar{S} \approx 0.2$  commonly used axial clearance the clocking effect can be clearly seen in high-loaded stages of an axial compressor and is a persistent physical phenomena in turbomachines. At present, it is found that optimization of clocking position of blade rows is an efficient way to control the unsteady interactions between rows in a multistage turbomachine and can be used in operational development or design of compressors.

### Conclusions

1. A series of experimental studies for three versions of a high-loaded first Stage A-1 of a few-stage HPC for an engine core demonstrator is completed to optimize the control program and analyze the effect of casing treatment (CT No.2) and "clocking" effect on parameters and characteristics of the Stage with the following design values:  $G_{A\text{ cor}}=24.4$  kg/s;  $\pi^*=2.28$ ;  $U_{c.\text{cor}}=421$  m/s;  $\bar{d}_1=0.6623$ .

2. Optimal IGV and Stator control program providing high efficiency of the Stage ( $\eta^*_{ad}=0.88\div 0.89$ ) at  $\bar{n}_{cor}=0.6\div 0.95$  is found and tested. An increase in  $\bar{n}_{cor}$  up to 1.0 results in a decrease in efficiency. The stall margin from the optimal point to stall at  $\bar{n}_{cor}=0.7$  is  $\Delta SM=23\%$ , and then decreases down to  $\Delta SM=17\%$  at  $\bar{n}_{cor}=0.95$  or  $\Delta SM=12\%$  at  $\bar{n}_{cor}=1.0$ .
3. Application of casing treatment results in an increase in the stall margin by 12% within  $\bar{n}_{cor}=0.6\div 0.9$  with a simultaneous increase in efficiency by  $\sim 3\%$ .
4. Clocking effects in Stage A-1 are moderate (efficiency changes by 0.7%) due to high axial clearances between rows.

### References

- [1] Savin N.M., and Saren V.E. "Effects of stator clocking in system of rows stator-rotor-stator of the subsonic axial compressor. Unsteady aerodynamics, aeroacoustics and aeroelasticity of turbomachines". Eds. K.C. Hall, R. Kielb, and J.P. Thomas. Dordrecht, the Netherlands: Springer. 581-601, 2006.
- [2] Savin N.M., and Saren V.E. "Gasdynamic effects of tangential bowing of stator vanes in a subsonic stage of axial compressor". *Turbomachines aeroelasticity aeroacoustics unsteady aerodynamics*. 201-214, 2006.
- [3] V.I. Mileshin, "Challenges in fan and high pressure compressor development". *ISABE2013*, Invited Paper ISABE2013-1003, Busan, South Korea, 2013.
- [4] Mileshin V.I., Brailko I.A., Savin N.M., Kozhemyako P.G. Numerical and Experimental Analysis of Rotor and Stator Clocking Effect by Example of Model High Loaded Two Stage Compressor on  $\pi^*c=3.7$ . Proceedings of ISABE conference 2013, paper ISABE-2013-1131.
- [5] F.Sh. Gelmedov, V.I. Mileshin, P.G. Kozhemyako, I.K. Orekhov. "Stall margin improvement in three-stage Low pressure compressor by use of slot type casing treatments". Proceedings of ASME TURBO EXPO 2014, Paper GT2014-26298, Dusseldorf, Germany, 2014.
- [6] V.I. Mileshin, N.M. Savin, P.G. Kozhemyako, Ya.M. Druzhinin. "Numerical and experimental analysis of radial clearance influence on rotor and stator clocking effect by example of model high loaded two stage compressor". Proceedings of ASME TURBO EXPO 2014, Paper GT2014-26345, Dusseldorf, Germany, 2014.
- [7] V.I. Mileshin, Stepanov A.V., N.M. Savin, Ya.M. Druzhinin. "Numerical and experimental Investigations of Clocking Effect in a two-stage compressor with  $\pi^*c=3.7$ ". Proceedings of ASME TURBO EXPO 2015, Paper GT2015-43472, Dusseldorf, Germany, 2015.
- [8] V.I. Mileshin, I.A. Brailko, A.V. Stepanov, V.N. Korzhnev. "Numerical and Experimental Investigations of Steady and Unsteady Characteristics of a Counter Rotating Fan Model with Thickened Blades of Working Wheel". *Proceedings of ASME TURBO EXPO 2012*, Paper GT2012-69734, Copenhagen, Denmark, 2012.
- [9] F.Sh. Gelmedov, Eu.I. Stepanov, S.A. Smirnov. "Aerodynamics of Stage K-11 - a typical high-loaded first stage for a turbofan high-pressure compressor". CIAM 2001-2005, Fundamental results of research, development, and engineering works, v. 1, pp. 298-251.
- [10] Hsu, S. T. and Wo, A. M., "Reduction of Unsteady Blade Loading by Beneficial Use of Vortical and Potential Disturbances in an Axial Compressor with Rotor Clocking," Proceedings of ASME TURBO EXPO 1997, 97-GT-86, 1997.
- [11] He, L., Chen, T., Wells, R. G., Li, Y. S., and Ning, W. "Analysis of Rotor-Rotor and Stator-Stator Interferences in Multi-Stage Turbomachines". Proceedings of ASME TURBO EXPO 2002, GT-2002-30355, 2002.
- [12] Kato, D., Imanari, K. "Effects of Airfoil Clocking on Aero-Performance and Unsteady Blade Loading in a High-Speed Axial Compressor". Proceedings of the International Gas Turbine Congress IGTS2003, Paper TS-058, Tokyo, Japan, 2003.
- [13] J. Stading, J. Friedrichs, T. Waitz, C. Dobriloff, B. Becker, V. Gummer. "The Potential of Rotor and Stator Clocking in a 2.5-stage Low-speed Axial Compressor". Proceedings of ASME TURBO EXPO 2012, Paper GT2012-68353, Copenhagen, Denmark, June 2012.
- [14] Barankiewicz, W.; Hathaway, M. Effects of Stator Indexing on Performance in a Low Speed Multistage Axial Compressor, Proceedings of ASME TURBO EXPO 1997, 97-GT-496, 1997.